

INVESTIGATION OF CARBON STEEL AND STAINLESS STEEL CORROSION IN A MEA BASED CO₂ REMOVAL PLANT

Amir Erfani¹, Saeed Boroojerdi^{2*}, Ashraf Dehghani², Mohammad Yarandi²

¹*School of Chemical, Gas and Petroleum Engineering, Semnan University, Semnan, Iran*

²*Process and Equipment Technology Development Division, Research Institute of
Petroleum Industry, Iranian Oil Company, Tehran, Iran*

Received September 22, 2014, Accepted January 30, 2015

Abstract

Corrosion is highly problematic in operation of CO₂ removal units. In this research, linear polarization resistance method, corrosion coupon experiments, weight loss tests in pilot and light microscopy were utilized to demonstrate and give a better understanding of corrosion problems in this plant. Effect of temperature, corrosion inhibitor and CO₂ content on carbon steel and stainless steel were analyzed in both laboratory and long duration tests in operating plant. Experimental results show that in lean amine solution, temperature change from 60 °C to 80 °C, increases carbon steel corrosion rate from less than 1milli-inch per year (mpy) to 11 mpy, while in rich amine, corrosion rate is less affected by temperature. A commercial blend of salicylic acid is utilized as a corrosion inhibitor and can inhibit carbon steel corrosion rate by 43%.

Key words: Linear polarization resistance; Corrosion inhibitor; Carbon steel; Weight loss measurements; CO₂ corrosion.

1. Introduction

Steel CO₂ induced corrosion and inhibition has been an important topic in petroleum industry [1-2]. Amines have been utilized for removal of CO₂ or H₂S in gas refineries or other gas sweetening applications for decades [3-5]. Moreover many researchers have explored optimum amine for a specified application to obtain better performance [2,6-8]. Corrosion is one of the major concerns facing the main equipments after some years of working of these units. Thus, it is one of criteria's in selecting solvent, piping material and optimizing operating conditions [9-14]. Different CO₂ removal units deal with different CO₂ content in feed gas. For CO₂ capture in fossil fuel power plants, gas-fired flue gases and coal-fired flue gas typically contain 8% and 13% CO₂, respectively. A typical natural gas processing unit sour gas contains 1% H₂S and 3% CO₂. The syn-gas in ammonia process typically contain 18% molar CO₂, which is higher than all typical CO₂ removal applications which can make the corrosion even more problematic. Some researches focus on evaluation of corrosion inhibitor effectiveness to lower corrosion problems [15-17]. Corrosion inhibitors can play a major role in decreasing corrosion rate [18-19].

Since corrosion is an electrochemical reaction, the electrochemical measurements are highly used in corrosion investigations. Linear Polarization Resistance (LPR) Probes are compatible for electrolyte systems, so that they can be utilized in electrochemical corrosion tests for amine systems. Furthermore, corrosion coupons can be utilized both for quantitative estimation of average corrosion rate and visual indication of corrosion type in an industrial unit.

The process flow of CO₂ separation from feed gas is illustrated in Fig. 1. In a petrochemical complex, for absorption of acid gas containing about 17% molar CO₂, 25%wt MEA is utilized in two steps of absorption and stripping. High pressure absorption of acid gas in absorption (T-101) and stripping tower with pressure reduction in (T-102 A/B) towers are achieved. After CO₂ separation from feed gas, CO₂ is sent to urine unit. The feed gas enters the absorption tower from bottom and lean amine is introduced from top. When the solvent

becomes rich with acid gas, it needs to be recovered. After the rich solvent leaves the absorption tower, it passes through E-101 heat exchanger (known as L/R exchanger) and is heated. After passing through pressure reduction valve, some of the acid gas is stripped and enters reboiled stripper T-102 A/B. In this tower all acid gas is stripped and lean solvent goes into L/R exchanger and then pumped back to the top of the absorption tower. Specifications of feed and sweet gas are presented in Table 1.

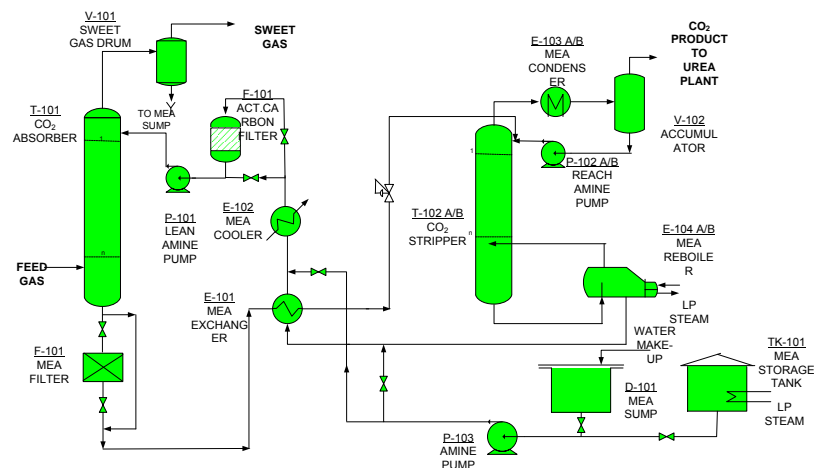


Fig. 1 CO₂ acid gas removal process flow

Plant corrosion report shows that uniform, localized, pitting and galvanized corrosion are common in described plant. Dead zones and locations with highest temperature are the most probable pitting corrosion locations. Galvanic corrosion is common in connection of stainless steel valves and carbon steel pipes. Industrial corrosion report show that stress cracking corrosion (SCC) is common in heat exchangers and absorber tower and is usually seen in stainless steel welded joints; therefore, stress relieving in welding is absolutely essential. Reports show severe corrosion in 101 and 102 heat exchangers. In 101 heat exchanger lean amine pass shell while rich amine passes tubes.

Corrosion inhibitors can play a major role in decreasing corrosion rate on the basis of the three known mechanisms: creating protective film on metal surface, creating protective oxide layer on metal surface and change in pH or reaction with corrosive components.

The aim of this research is to demonstrate effect of temperature, corrosion inhibitor and dissolved CO₂ on corrosion of the system. We had the opportunity not only to perform LPR tests but also to obtain long duration coupon corrosion data in an operating CO₂ removal unit.

2. Experimental

All electrochemical tests were carried out according to ASTM G1, G5-94 and ASTM G3 to obtain reliable data which include preparing, cleaning, and evaluating corrosion test specimens [20-22].

2.1 Linear polarization resistance (LPR)

The benefit of electrochemical measurement is its short measurement time. LPR measurements were carried out by using Potentiostat/Galvanostat EG&G 237Autilizing M352 software. Three electrodes system were used in these experiments. Two graphite electrodes as counter electrode, calomel-saturated electrode (CSE) as reference electrode and carbon steel or stainless less steel as working electrode were used. Working electrode has a surface area of 5 cm². Chemical analysis of carbon steel electrode is presented in Table 1.

Before polarization experiment, the open circuit potential (OCP) measurements were taken until the stability was reached. Potentio-dynamic polarization curves were then obtained at 1 mV/sec scanning rates covering a potential range of ± 300 mV around the free corrosion potential. The corrosion rate was determined later by using Tafel extrapolation method. Experiments were in range of 60°C to 80°C. Amine solution was obtained from

under study industrial plant. CO₂ were used for saturation of amine for rich amine experiments.

Table 1 Chemical analysis of carbon steel (%wt.)

| | | | | | | | |
|-------|-------|-------|--------|-------|-------|--------|-------|
| Fe | C | Si | Mn | Cr | Mo | Ni | Al |
| 97.97 | 0.184 | <0.05 | 1.588 | 0.037 | 0.107 | 0.02 | <0.01 |
| Co | Cu | Nb | Ti | V | W | Zr | Pb |
| <0.02 | 0.034 | 0.011 | <0.005 | 0.005 | <0.04 | <0.003 | <0.01 |

2.2. Corrosion coupon experiments

Average corrosion rate measurements were carried out by using metal coupons. Coupons were installed in working plant for 2000 hours. After removing coupons from plant streams, coupons were dried and cleaned and weighed. Corrosion rate were calculated according to difference in mass. For average corrosion rate measurements, carbon steel (AISI 1020) and stainless steel 316 coupons were installed in 3 designed loops. These loops were located at 108 heat exchanger, 109 heat exchanger and amine sump. According to ASTM G1, corrosion rate were calculated as follows:

$$\text{Corrosion rate (mpy)} = \frac{3.45 \times 10^6 \times W}{A \times T \times D}$$

mpy: milli-inch per year; W: mass loss (gr); A: coupon surface area (cm²); T: exposure time (h); D: density (gr/cm³).

Density of carbon steel and stainless steel 316 were considered 7.86 gr/cm³ and 7.98 gr/cm³, respectively.

2.3. Pilot plant weight loss investigations

Rich and lean amine solution with and without inhibitor were investigated in high pressure vessels. Weight loss method was integrated to obtain corrosion rate of carbon steel and stainless steel 316 with surface areas of 25 cm². CO₂ was used for pressurizing vessel to 20 bar gauge. Experiments were carried out at 64°C. For chemical analysis, two samples were collected from lean and rich amine streams. Table 2 presents gathered data.

Table 2 Chemical analysis of collected plant rich and lean amine samples

| solution | pH (25°C) | MEA concentration (% wt.) | Cl ⁻ concentration (ppm) |
|----------|--------------|------------------------------|--|
| Rich MEA | 8 | 19 | <1 |
| Lean MEA | 11 | 18 | <1 |

Amine degradation plays a major role in corrosion rate. Two samples from lean and rich amine were collected to be analysis for degraded amines. Results show degradation in lean amine stream was 1.5% and in rich amine was 1.2%.

3. Results and discussion

3.1. Linear polarization resistance investigations

3.1.1 Effect of temperature in lean, rich and saturated solutions

Fig. 2 and Fig. 3 illustrate polarization curves of carbon steel in lean and rich amine at two different temperatures. These polarization curves shows that for lean amine temperature change can highly change corrosion rate of carbon steel. On the other hand, for rich amine this temperature change had minor effects. Table 3, presents corrosion rate and potential for these systems.

Table 3 Corrosion potential and rate of carbon steel in rich amine solution

| Solution | Temperature (°C) | Corrosion potential (mV) vs SCE | Corrosion Rate (mpy) |
|------------|---------------------|------------------------------------|-------------------------|
| Lean Amine | 60 | -708 | <1 |
| | 80 | -909.6 | 11.86 |
| Rich Amine | 60 | -860.5 | 10.20 |
| | 80 | -888.6 | 12.21 |

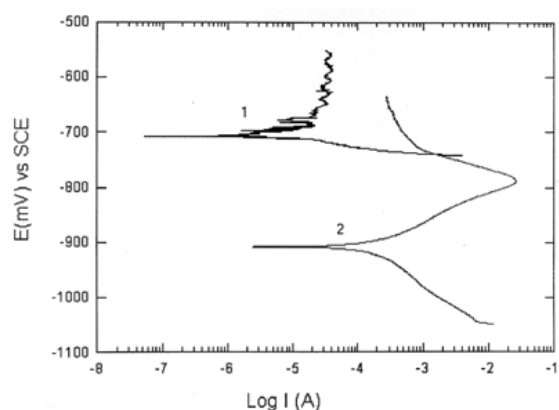


Fig. 2 Polarization curves of carbon steel in lean amine at (1): 60°C and (2): 80°C

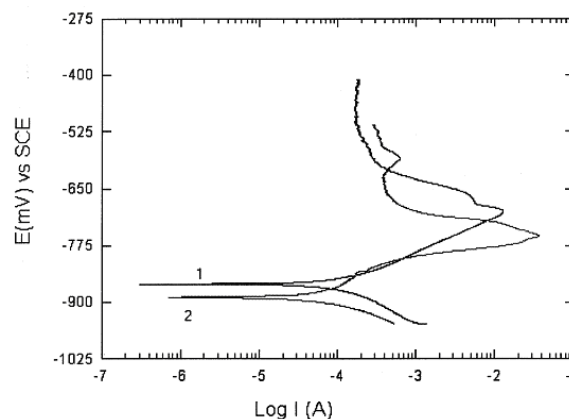


Fig. 3 Polarization curves of carbon steel in rich amine at (1): 60°C and (2): 80°C

Effect of CO₂ in amine solution is described by following reactions:

Carbamate formation:



Carbamate hydrolysis:



Corrosion reaction:

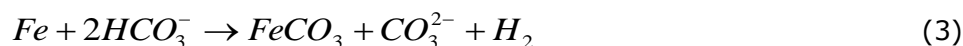


Fig. 4 illustrates polarization curves of carbon steel in CO₂ saturated amine solution. CO₂ has increased corrosion rate and lower the anodic potential, temperature difference has a minor effect. Table 4 presents corrosion rate and potential for these experiments.

Table 4 Corrosion rate of carbon steel in CO₂ saturated rich amine solution

| Temperature (°C) | Corrosion potential (mV) vs. SCE | Corrosion rate (mpy) |
|------------------|----------------------------------|----------------------|
| 60 | -851.6 | 12.23 |
| 80 | -864.1 | 12.51 |

3.1.2 Effect of Corrosion inhibitor in CO₂ saturated rich amine

The most important parameter that shows an inhibitor is effective for an application is inhibitor efficiency. The efficiency of an inhibitor is expressed by decreasing corrosion rate. Thus it is expressed as:

$$\text{Inhibitor Efficiency} = \left[1 - \frac{CR_{\text{inhibited}}}{CR_{\text{uninhibited}}} \right] \times 100\%$$

in which CR_{inhibited} stands for corrosion rate in presence of inhibitor and CR_{uninhibited} stand for corrosion rate in blank solution. In this work, commercial inhibitor Corrate 12Z from Betz Dearborn was investigated. Inhibitor was tested in rich amine solution saturated with CO₂ at 80 °C and the results are presented in Table 5. With respect to these data, this inhibitor reaches highest efficiency at 200 ppm. Fig 5 illustrates polarization curves of 200 ppm solution and compares them to blank solution.

Table 5 Corrosion inhibition in rich amine solutions at 80°C

| Inhibitor concentration (ppm) | Corrosion potential mV vs. SCE | Corrosion rate (mpy) | Inhibitor efficiency (%) |
|-------------------------------|--------------------------------|----------------------|--------------------------|
| - | -851.6 | 12.51 | |
| 100 | -795.1 | 7.093 | 43.26 |
| 200 | -818.5 | 7.089 | 43.33 |
| 400 | -814.2 | 8.99 | 28.1 |
| 800 | -837.7 | 7.7 | 38.45 |
| 1000 | -841 | 9.2 | 26.45 |

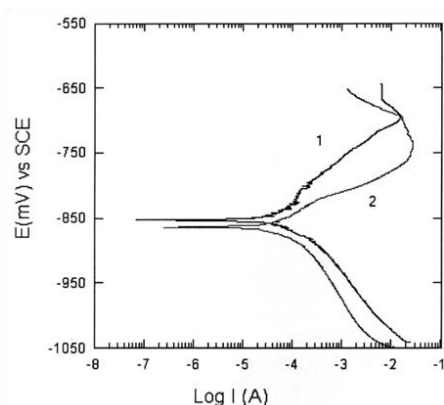


Fig. 4 Polarization curves of carbon steel in rich amine saturated with CO₂ at (1): 60°C and (2): 80°C

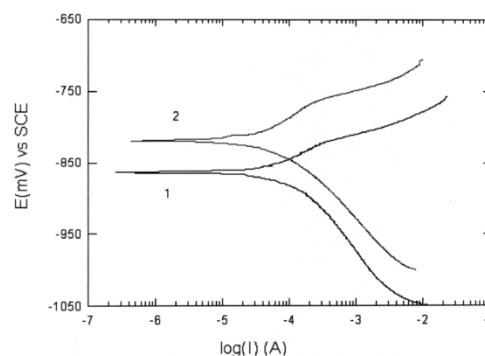


Fig. 5 Rich amine polarization curve at 80°C (1): without inhibitor (2): 200ppm inhibitor

3.1.3. Effect of Corrosion inhibitor in lean amine solution

Fig. 6 illustrates polarization curves for lean amine solution with and without corrosion inhibitor, at 80°C. Results show that described inhibitor can also reduce corrosion rate in lean amine solution from 11.86 mpy to 8 mpy.

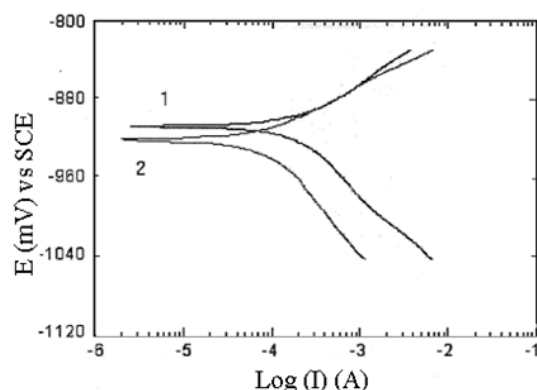


Fig. 6 Lean amine polarization curve at 80°C 1: without inhibitor, 2: 200ppm inhibitor

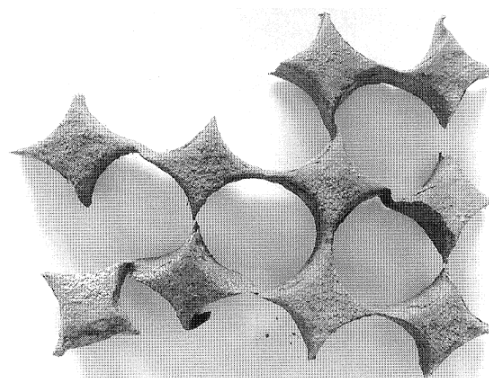


Fig. 7 Corroded part of heat exchanger tube sheet

3.2. Corrosion coupon investigations

Table 6, summarizes the results of corrosion coupons. Results show that both Carbon steel and stainless steel 316 have a corrosion rate less than 5 mpy.

Table 6 Corrosion coupon investigation results

| Coupon exposure location | Alloy | Mass difference | Exposure time (hr) | Area (cm ²) | Corrosion rate (mpy) | General observations |
|--------------------------|--------|--|--------------------|-------------------------|----------------------|--|
| 101 heat exchanger | CS | 0.2343 | 2009 | 12.93 | 3.95 | General corrosion |
| | CS | 0.2162 | 2009 | 12.93 | 3.65 | General corrosion |
| 102 heat exchanger | CS | 0.3469 | 2009 | 16 | 4.73 | General corrosion, Black corroded film |
| | CS | 0.012 | 646 | 10.73 | 0.676 | Not corroded |
| | CS | This coupon have been in place in contact with heat exchanger shell (stainless steel) and has been completely corroded due to galvanic corrosion | | | | |
| | SS 316 | This coupon was broken due to mechanical tensions | | | | |
| Amine Sump | CS | 0.2259 | 1993 | 24.43 | 2.036 | General corrosion Black corroded film |
| | SS 316 | 0 | 1993 | 18.08 | 0 | Not corroded |

3.3. High pressure pilot weight loss investigations

Experiment specifications and results for pilot plant weight loss experiments are summarized in Table 7. Tests show that average corrosion rate of stainless steel 316 in rich amine is 80% lower than carbon steel.

Table 7 Corrosion rate results for carbon steel and stainless steel 316, pilot plant data at 20 bar gauge and 64°C

| Solution | Alloy | Exposure time (hr) | Corrosion rate (mpy) |
|---------------------------------|---------------------|--------------------|----------------------|
| Rich Amine (Blank) | Carbon steel | 500 | 0.853 |
| | Carbon steel | 500 | 0.344 |
| | Carbon steel | 360 | 0.53 |
| | Stainless steel 316 | 500 | 0.197 |
| | Stainless steel 316 | 360 | 0.043 |
| Lean Amine (Blank) | Carbon steel | 500 | 0.00 |
| Rich Amine + 50 PPM inhibitor | Carbon steel | 360 | 0.18 |
| | Stainless steel 316 | 360 | 0.00 |
| Rich Amine + 500 PPM inhibitor | Carbon steel | 500 | 0.7 |
| | Carbon steel | 500 | 0.488 |
| | Stainless steel 316 | 500 | 0.00 |
| Rich Amine + 1000 PPM inhibitor | Carbon steel | 500 | 1.5 |
| | Carbon steel | 500 | 1.08 |
| Lean Amine + 500 PPM inhibitor | Carbon steel | 500 | 2.02 |
| | Carbon steel | 500 | 0.5 |
| | Carbon steel | 500 | 0.54 |

3.4. Micro structure evaluations of heat exchanger tube sheet

A small metal sample from heat exchanger tube sheet is illustrated in Fig. 7; this corroded sample is investigated using light microscopy for evaluation of its microstructure. Fig. 8 and Fig. 9 illustrate optical micrograph of metal surface. Nital 2% is used for etching the samples. After investigations on sample edge shows uniform corrosion of sample which has been confined within the grains.

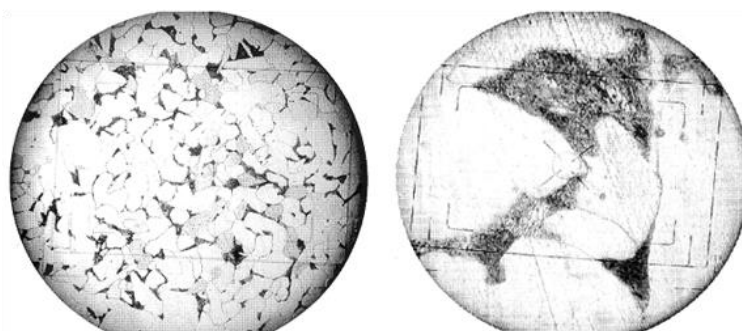


Fig. 8 Optical micrograph of Ferrite-pearlite microstructure, left: 100X magnification, right: 1500X magnification

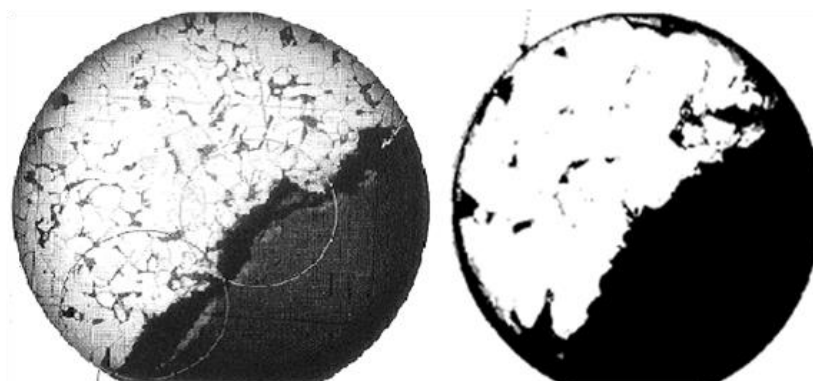


Fig. 9 Optical micrograph of studied sample edge, general corrosion, left: 200X magnification, right: 500X magnification

4. Summary and Conclusions

In this study, LPR method, Corrosion coupon experiments, pilot weight loss test and light microscopy were utilized to demonstrate and solve corrosion problems of and industrial plant. Our study reports:

- LPR experiments shows that studied corrosion inhibitor can best inhibit rich amine corrosion at 200 ppm concentration. At this concentration inhibitor efficiency is 43.33% and carbon steel corrosion rate is 7.089 mpy. Corrosion inhibitor increase corrosion potential to more positive potentials about 40mv.
- In lean amine solution, temperature change from 60°C to 80°C increase carbon steel corrosion rate from less than 1mpy to 11 mpy.
- In rich amine corrosion rate is less affected by temperature and a temperature change from 60°C to 80°C increase corrosion rate from 12.23 mpy to 12.51 mpy.
- Corrosion coupon investigations shows that average corrosion rate for both carbon steel and stainless steel 316, in studied unit is less than 5 mpy.
- Pilot plant tests show that average corrosion rate of stainless steel 316 in rich amine is 80% lower that carbon steel.
- Uniforms corrosion was the main corrosion mechanism in studied samples

References

- [1] Zettler, H. U., H. Müller-Steinhagen, and B. Hedges. "Modification of carbon steel surfaces to reduce corrosion fouling in oil and gas industry." *Petroleum Science and Technology* 21, (3-4), 2003, 681-698.
- [2] Jingen, D., Y. Wei, L. Xiaorong, and D. Xiaoqin. "Influence of H₂S content on CO₂ corrosion behaviors of N80 tubing steel." *Petroleum Science and Technology* 29, (13), 2011, 1387-1396.
- [3] Kohl, A. L., and R. B. Nielsen. "Gas purification 5th ed." *Houston: Gulf Publishing Company* (1997).
- [4] Maddox, Robert Nott. *Gas and Liquid Sweetening*. M. Campbell, 1974.
- [5] Pourjazaieri, S., M. Zoveidavianpoor, and S. R. Shadizadeh. "Simulation of an Amine-based CO₂ Recovery Plant." *Petroleum Science and Technology* 29 (1), 2011, 39-47.
- [6] Rochelle, Gary T. "Amine scrubbing for CO₂ capture." *Science* 325, no. 5948 (2009), 1652-1654.
- [7] Polasek, J. C., J. A. Bullin, and S. T. Donnelly. "How to reduce costs in amine-sweetening units." *Chem. Eng. Prog.;(United States)* 79 (1983).
- [8] Yang, Jingyi, Xinru Xu, and Shaozhou Chen. "Selective Removal of H₂S from Petroleum Refinery Gases. III. A Study on the Corrosion in Desulfurizer-H₂S-CO₂-H₂O System." *Petroleum Science and Technology* 21, (1-2), 2003, 29-42.
- [9] Rooney, Peter C., and Michael C. DuPart. "Corrosion in alkanolamine plants: causes and minimization." *CORROSION 2000* (2000).
- [10] Bonis, M., J. P. Ballaguet, and C. Rigai. "A critical look at amines: a practical review of corrosion experience over four decades." In *83rd Annual GPA Convention, New Orleans*. 2004.
- [11] DuPart, M. S., T. R. Bacon, and D. J. Edwards. "Understanding corrosion in alkanolamine gas treating plants." *Hydrocarbon Processing* 72, no. 5 (1993): 89-94.
- [12] Gouedard, C., D. Picq, F. Launay, and P-L. Carrette. "Amine degradation in CO₂ capture. I. A review." *International Journal of Greenhouse Gas Control* 10 (2012): 244-270.
- [13] Blanc, C., M. Grall, and G. Demarais. "Part played by degradation products in the corrosion of gas sweetening plants using DEA and MDEA." In *Proc. Gas Cond. Conf.; (United States)*, no. CONF-8203176-. 1982.
- [14] Veawab, Amornvadee, Paitoon Tontiwachwuthikul, and Sanjiwan D. Bhole. "Studies of Corrosion and Corrosion Control in a CO₂-2-Amino-2-methyl-1-propanol (AMP) Environment." *Industrial & engineering chemistry Research* 36 (1), 1997, 264-269.
- [15] Sastri, Vedula S. *Corrosion inhibitors: principles and applications*. New York: Wiley, 1998.

- [16] Veawab, Amornvadee, Paitoon Tontiwachwuthikul, and Amit Chakma:. "Investigation of low-toxic organic corrosion inhibitors for CO₂ separation process using aqueous MEA solvent." *Industrial & Engineering Chemistry, Research* 40, no. 22 (2001): 4771-4777.
- [17] Barham, H. A., S. A. Brahim, Y. Rozita, and K. A. Mohamed. "Carbon steel corrosion behaviour in aqueous carbonated solution of MEA/bmim DCA." *International Journal of Electrochemical Science* 6, no. 1 (2011): 181-198.
- [18] Wang, Y., D. Han, D. Li, and Z. Cao. "A Complex Imidazoline Corrosion Inhibitor in Hydrochloric Acid Solutions for Refinery and Petrochemical Plant Equipment." *Petroleum Science and Technology* 27 (16), 2009, 1836-1844.
- [19] El-Sukkary, M. M. A., I. Aiad, A. Deeb, M. Y. El-Awady, H. M. Ahmed, and S. M. Shaban. "The Preparation and Characterization of Some Novel Quaternary Iminium Salts Based on Schiff-base as a Corrosion Inhibitor." *Petroleum Science and Technology* 28, (11), 2010, 1158-1169.
- [20] ASTM G1-03. "Standard practice for preparing, cleaning, and evaluating corrosion test specimens." (2003).
- [21] ASTM G3-89. "Standard Practice for Conventions Applicable to Electrochemical Measurements in Corrosion Testing." (2010).
- [22] ASTM G5. "Standard Reference Test Method for Making Potentiostatic and Potentiodynamic Anodic Polarization Measurements", (2004).